EPJ Web of Conferences **134**, 04003 (2017) DOI: 10.1051/epjconf/201713404003
Subnuclear Structure of Matter: Achievements and Challenges

Study of QCD-dynamics in η and η' production and decays

Reinhard Beck[1,⋆] and *Ulrich* Wiedner[2,⋆⋆]

[1] *Helmholtz-Institut für Strahlen- und Kernphysik, Rheinische Friedrich-Wilhelms-Universität Bonn, Nußallee 14-16, 53115 Bonn*
[2] *Institut für Experimentalphysik I Ruhr-Universität Bochum Universitätsstraße 150, 44780 Bochum*

Abstract. One aim of this project lies in studying QCD dynamics using photoproduction of η and η' mesons with the CBELSA/TAPS experiment at the accelerator facility ELSA. Hadronic decay modes of η and η' are analyzed that allow the study of symmetry breaking effects in QCD. Furthermore, excited η-states produced with a photon beam are studied within the scope of this project. Of special interest is hereby the nature of the $\eta(1405)$. The high data samples for η- and η'-photoproduction off the proton allow in addition the determination of polarization observables.

1 Introduction

The scientific goal of this project is the study of QCD dynamics in the photoproduction of pseudoscalar and vector mesons and their subsequent decay pattern. Especially in focus are the ground-state η and η' mesons and excited η states. Various decays of the η and η' are forbidden by conservation laws. For example, the hadronic decay modes $\eta \to 3\pi$ only occur due to the isospin-violating quark-mass difference $m_u - m_d$ or due to electromagnetic effects, and the decays $\eta, \eta' \to \pi\pi\gamma$ are sensitive to the QCD box anomaly. A systematic study of such decays offers a way to investigate symmetries and symmetry breaking effects in QCD (see project B.3). The second goal within the project is related to the question of the production cross-section of excited η-states with a photon beam. In particular, the nature of the $\eta(1405)$, discovered in antiproton-proton annihilation, has been discussed extensively and controversially in the literature. It is considered as a good candidate for the pseudoscalar glueball, even though its mass is significantly lower than lattice calculations predict. Recent studies of $\eta(1405)$ decays did lead to unexpected results, thus adding to the ambiguity in the interpretation of its nature. More light on the nature of the $\eta(1405)$ can be shed by studying the processes that lead to its production. While the $\eta(1405)$ is clearly produced in gluon-rich processes like radiative J/Ψ decays or antiproton-proton annihilation, the production cross section with a photon beam is unclear. Data from the CBELSA/TAPS experiment give only a very weak signal for the production of the $\eta(1405)$ – perhaps an indication for a gluonic nature of the particle, because glue is not expected to be produced copiously by photon beams. However, the statistical evidence does not allow any decisive conclusion. In addition, we are carrying out analyses of the production of $\eta(1405)$ in radiative J/ψ and ψ' decays measured with the BES III detector in Beijing and in antiproton-proton annihilation at different momenta. The latter data were taken with the Crystal Barrel detector at the LEAR accelerator at CERN.

⋆ e-mail: beck@hiskp.uni-bonn.de
⋆⋆ e-mail: wiedner@ep1.rub.de

2 Project Results

2.1 Determination of the Dalitz plot parameter α and precise measurement of the η mass

The Dalitz plot parameter α for the $\eta \to 3\pi^0$ decay was precisely measured, see the PhD-thesis of M. Unverzagt [1] and [2, 3]. The experiment was performed with the Crystal Ball and TAPS large acceptance photon detectors at the tagged photon beam facility of the MAMI-B electron accelerator in Mainz. High statistics of $1.8 \cdot 10^6$ $\eta \to 3\pi^0$ events were obtained, giving the result $\alpha = -0.032 \pm 0.002_{\text{stat.}} \pm 0.002_{\text{syst.}}$ which is presented in Fig. 1(a). The most recent values for the slope parameter are: $\alpha = -0.044 \pm 0.004$ [5], $\alpha = -0.025 \pm 0.004$[6], $\alpha = -0.0302 \pm 0.0011$[7].

In addition, a new precise determination of the η meson mass was performed, see the PhD-thesis of A. Nikolaev [8] and [9]. It is based on a measurement of the threshold for the $\gamma p \to p\eta$ reaction using the tagger focal-plane microscope detector at the MAMI-B facility in Mainz. In Mainz the real photon beam was produced by bremsstrahlung of the 883 MeV electrons from MAMI-B [10, 11] on a 100 μm thick diamond radiator. The absolute electron energy, E_0, of the incident beam was precisely determined [12, 13] in the third race-track microtron of MAMI-B with a total uncertainty of about $\sigma_0 = 140$ keV. The photon energies were determined using the Glasgow photon tagging spectrometer (tagger) [14, 15], which provided a tagged photon flux of roughly $10^5\,\text{s}^{-1}\,\text{MeV}^{-1}$ at a beam current of about 35 nA.

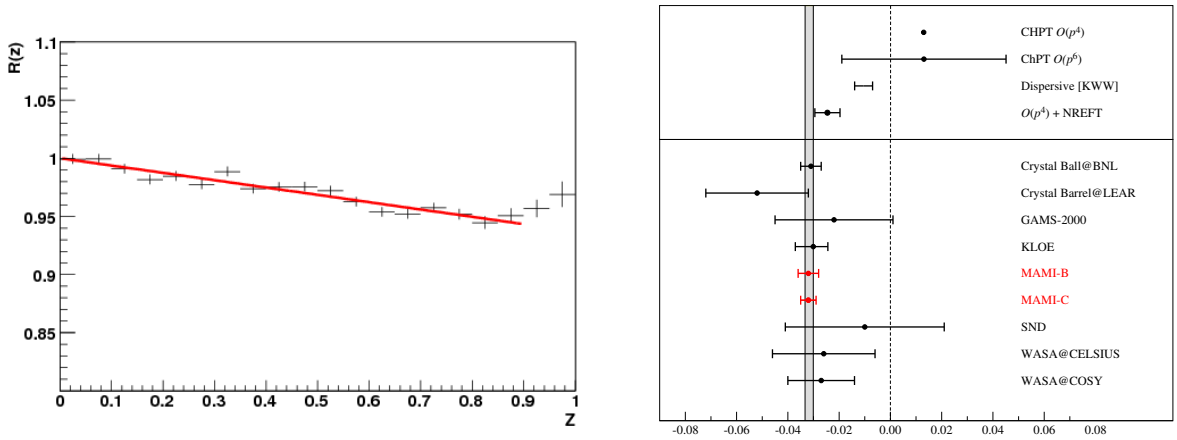

(a) (b)

Figure 1. (a) Ratio R(z) of the simulated and the measured z distributions. The Dalitz plot parameter, α, was obtained directly from the fit of the function $c(1 + 2\alpha z)$ (red line). (b) World data and prediction for the slope parameter α (PDG 2010 value shaded gray) [4] and the new precise α values from MAMI-B [2] and MAMI-C [3].

For the first time the tagger focal-plane microscope detector [16] was used to improve the tagged photon energy resolution. The microscope detector was placed in front of the main focal-plane spectrometer (see Fig. 2(a)), so that it covered the region around the η production threshold ($E_{\text{thr}} \approx 707\,\text{MeV}$) from $E_\gamma = 674\,\text{MeV}$ to $E_\gamma = 730\,\text{MeV}$ at an electron beam energy $E_0 = 883\,\text{MeV}$. Made of 96 scintillator strips overlapping to one third, it provided 191 tagging channels with a higher energy resolution of about 0.29 MeV per channel compared to approximately 1.8 MeV available from the main focal-plane detector.

The 4.76 cm long liquid hydrogen target was located at the center of the Crystal Ball photon spectrometer. The Crystal Ball [17, 18], covering polar angles between $\theta = 20°$ and $\theta = 160°$, consisted of 672 NaI(Tl) crystals (see Fig. 2(b)) and had two openings for the beam in forward and backward directions. Each NaI(Tl) crystal had the form of a truncated 41 cm long pyramid and was equipped with an individual photomultiplier. In order to distinguish between neutral and charged particles detected by the Crystal Ball, the system was equipped with a particle identification detector (PID) [19]. The PID was a cylindrical detector, consisting of 24 plastic scintillator strips of 2 mm thickness, arranged parallel to the photon beam axis.

The forward wall detector, TAPS [20], had 510 BaF_2 hexagonally shaped crystals, each equipped with a 5 mm thick plastic scintillator for identifying charged particles. A single BaF_2 crystal was 25 cm long and had an inner diameter of 5.9 cm. The TAPS detector, intended for detecting particles in the forward direction ($\theta = 4° - 20°$), was located at a distance of 173 cm from the Crystal Ball center, making it possible to use a time-of-flight analysis for the particle identification.

The experimental trigger comprised two levels. In the first level, the total energy deposited in the Crystal Ball was checked. If the sum of all photomultiplier analog signals exceeded a threshold corresponding to about 390 MeV, the event was accepted. The second-level trigger included a condition on the Crystal Ball sector multiplicity. The 672 crystals of the spectrometer were grouped into 45 sectors of up to 16 crystals each. If at least one of the 16 signals exceeded a threshold of 20 to 40 MeV, depending on the relative energy calibration of the photomultiplier signals, the sector contributed to the multiplicity. All events with multiplicity $M \geq 3$ and every third event with $M \geq 2$ were recorded for further analysis. The latter condition was used for the detection of the $\eta \to 2\gamma$ decay, while the first enhanced events from the six-photon decay.

The tagger microscope has a higher energy resolution than the standard tagging spectrometer and, hence, allowed an improvement in the accuracy compared to the previous η mass measurement at MAMI-B (see Fig. 3(a)). The result $m_\eta = (547.851 \pm 0.031_{\text{stat.}} \pm 0.062_{\text{syst.}})$ MeV agrees very well with the precise values of the NA48, KLOE and CLEO collaborations and deviates by about 5σ from the smaller, but also very precise value obtained by the GEM collaboration at COSY. A comparison of all current measurements is given in Fig. 3(b).

There were significant improvements in the η' event selection for the CBELSA/TAPS experiment, which is described in project A.1, especially concerning the $\eta' \to \pi^0\pi^0\eta$ channel, see the Diploma thesis of P. Nuhn [21]. This was achieved by implementing a kinematic fit and improvements in the background description. For every event, the kinematic fit returns a confidence level for the event hypothesis (in this case $\pi^0\pi^0\eta$). Rejecting events with a confidence level lower than 0.0001 eliminates a lot of background (cf. 5(a) red line). Without this cut the η'-peak would not be visible. The still considerable background stems from $3\pi^0$; it can be further reduced by using the kinematic fit with a $3\pi^0$-hypothesis and applying an anti-cut (cf. 5(a) blue line). The remaining background (cf. 5(b)) is attributed to further misidentified $3\pi^0$ final states and to direct $\pi^0\pi^0\eta$ production. For further analysis, it can be subtracted by methods such as multivariate

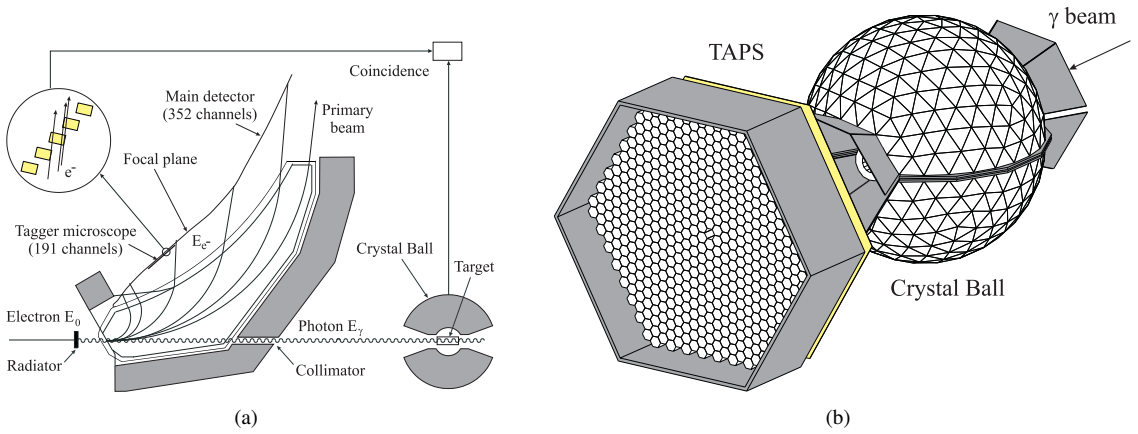

Figure 2. (a) Plan view of the tagging bremsstrahlung facility [14, 15] and the Crystal Ball detector (not to scale) at Mainz. The tagger microscope detector [16], giving improved resolution, was installed in the focal plane in front of the main detector at the position indicated. The inset shows the geometry of the microscope scintillators. (b) The Crystal Ball photon spectrometer and TAPS. The individual photomultipliers attached to the crystals are not shown; however, those supporting steel structures that were included in the Monte Carlo simulations are shown. Taken from [9].

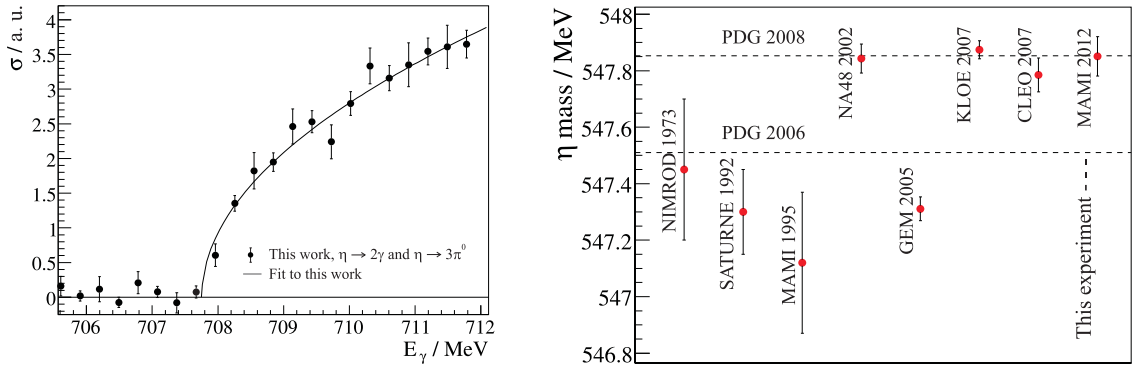

Figure 3. (a) Final results $\gamma p \to p\eta$ in the threshold region. (b) Overview of previous η mass measurements in comparison to the world average reported by the Particle Data Group in 2006 and 2008 (dashed lines) and the result of the new analysis [9].

side band subtraction or by determining the background contribution in each bin using a suitable fit function.

2.2 The double polarization observable E in η' photoproduction

Apart from the $\eta' \to \pi^0\pi^0\eta$ decay mode, the CBELSA/TAPS detector setup can be used to study the $\eta' \to \gamma\gamma$ decay mode with a branching ratio of only 2.2% as well. Both decay modes were analyzed in the Master thesis of F. N. Afzal [22, 23] with the aim to study baryon resonances by determining the double polarization observable E. Unlike the unpolarized cross section, polarization observables are sensitive to interference terms of multipoles and hence are sensitive to weakly contributing resonances, see project A.1. The η' meson has an isospin of $I = 0$, thus N* resonances with isospin $I = 1/2$ become exclusively accessible; Δ resonances can not contribute. Furthermore it is possible to investigate the high mass region ($m_{N^*} > 1890$ MeV) of the nucleon excitation spectrum due to the high mass of the η' meson (958 MeV). In this region many predicted but so far not observed N* states should be located. For the measurement of the double polarization observable E, a circularly polarized photon beam in combination with a longitudinally polarized butanol target was used. Fig. 5 shows the results for the double polarization observable E as a function of the photon beam energy. These results together with the already measured unpolarized cross section σ_0 data [24, 25] can be used to determine the helicity dependent cross sections $\sigma_{1/2}$ and $\sigma_{3/2}$ [23]. The positive sign of the double polarization observable E over the entire energy range of 1447 MeV - 2320 MeV indicate that the $A_{1/2}$ helicity amplitude is favored by the contributing resonances. For a complete disentanglement of all contributing resonances in this mass region more statistics and the measurement of more observables is needed however. In the future it is planned to take more data with a circularly polarized photon beam and a longitudinally polarized target with an electron beam of 3.2 GeV from ELSA.

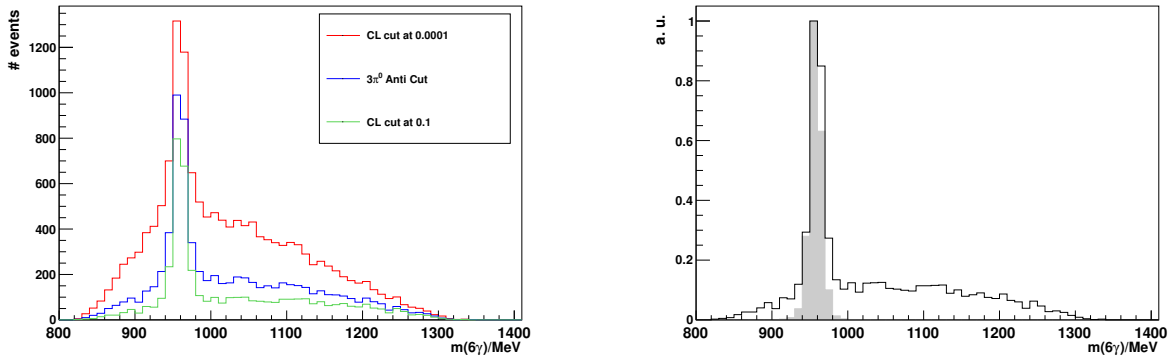

(a) (b)

Figure 4. (a) Cuts to improve η' event selection for 6γ final states (b) Comparison between Monte Carlo simulations (gray) and measured η' events.

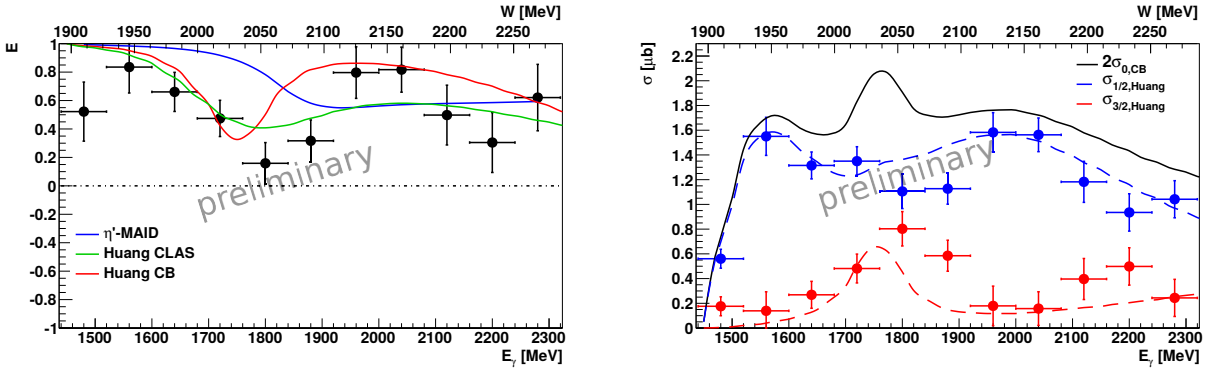

(a) (b)

Figure 5. (a)The double polarization observable E in η' photoproduction was determined in Master thesis of F.N. Afzal and is shown here as a function of the beam energy E_γ and the center of mass energy W. The data (black points) are compared to partial wave analysis predictions [27, 28].(b) The helicity dependent cross section $\sigma_{1/2}$ and $\sigma_{3/2}$ together with the fit to the unpolarized cross section $\sigma_0 = \frac{1}{2}(\sigma_{1/2} + \sigma_{3/2})$ data by [27]. Taken from [23].

2.3 Measurement of the beam asymmetry in η- and η'-photoproduction

From July to October 2013 the so far largest data sample for η- and η'-photoproduction off the proton with the CBELSA/TAPS experiment at ELSA was taken. An electron beam of 3.2 GeV from ELSA was incident on a thin diamond radiator. Linearly polarized photons were produced through coherent bremsstrahlung. The diamond radiator was oriented relative to the beam so that the coherent edge was located at 1750 MeV or at 1850 MeV, giving a maximum beam polarization degree of $p_\gamma = 40\%$ or 35% at 1750 MeV or 1850 MeV, respectively. As target a liquid hydrogen target of 10 cm thickness was chosen.

This beamtime can be used for several purposes, e.g. the determination of the beam asymmetry Σ in η and η'-photoproduction which is subject of an ongoing analysis. Within the energy range of 1100 MeV − 1800 MeV, $8.3 \cdot 10^6$ π^0 and $8.2 \cdot 10^5$ η events in the decay modes $\pi^0 \to \gamma\gamma$ and $\eta \to \gamma\gamma$ were selected [36] using kinematic cuts on the data. These events were used to determine the beam asymmetry Σ by fitting the ϕ-asymmetries $\Delta N(\phi)$ for each energy and angular bin:

$$\Delta N(\phi) = \frac{N_{-45^\circ} - N_{+45^\circ}}{N_{-45^\circ} + N_{+45^\circ}} = p_\gamma \Sigma \sin(2\phi), \qquad (1)$$

where N_{-45° and N_{+45° are the yields obtained with the polarization plane being at $\pm 45^\circ$ relative to the reaction plane, respectively and ϕ being the azimuthal angle of the selected meson in the final state. The preliminary results of the beam asymmetry Σ in η-photoproduction are shown in Fig. 6 for selected energy bins as a function of $\cos\theta$, where θ is the polar angle of the η meson in the center of mass system. The data are in good agreement with existing data from CB-ELSA [29] and GRAAL [30] (see Fig. 6(a) and 6(b)). Furthermore the different partial wave analyses (solutionsBnGa2014-01, BnGa2014-02 [35], the SAID-GE09 [34] and the JüBo2015 fit B [32]) agree well with the data since the existing data have been included in all solutions. Above 1500 MeV no data exist until now. Here our new data offer new input that will constrain the different partial wave analysis solutions which differ immensely at 1670 MeV (see Fig. 6(d)).

The beam asymmetry in η'-photoproduction has been measured so far only near the η' photoproduction threshold

for photon energies of 1461 MeV and 1480 MeV reported by the GRAAL collaboration [37]. These results show a zero crossing from positive to negative from forward to backward angles for both energy bins. This is surprising since near the η threshold, no such zero crossing was observed. This could indicate that the dynamics of η and η' photoproduction processes are different near threshold. With our collected data we will be able to extend the measured energy range for the beam asymmetry to 1800 MeV and investigate the dynamics of η and η' mesons further.
Another aim of this beamtime is the analysis of rare η and η' decays which will be done in future analyses. In addition it is possible to look for excited η states such as the $\eta(1405)$ using this and future beamtimes.

2.4 η-mesons and the quest for glueballs

The self-interaction of gluons that is central to QCD leads to a flux tube of gluons exchanged between the quarks that are bound by them. In consequence, quarks cannot be separated infinitely and are subject to confinement. It is a fact that individual free quarks have never been observed experimentally to date. The self-interaction in phenomenological models and in lattice gauge theory calculations clearly points to the existence of bound states of pure glue, known as glueballs.
Glueballs pose a very interesting facet of nature. The gluons are the mediator particles of the strong interaction and themselves massless. However, they do carry color, i.e., the charges of the strong interaction. It is generally believed that there is an attractive interaction between gluons leading for example in lattice calculations based on the QCD Lagrangian to a flux tube of gluons between the quark and the antiquark in a meson. The mutual gluon attraction should also allow for the formation of meson-like bound states of gluons, even if no quarks are present. Lattice calculations predict a whole spectrum of bound gluon states, the glueballs.
While the Higgs mechanism might be responsible for the masses of the elementary particles, the mass-creation mechanism for hadrons is quite different. Only a few percent of the mass of the proton is due to the Higgs mechanism. The rest is created, in a to date not very well determined way, by the strong interaction. In particular, glueballs themselves would be massless without the strong interaction and their predicted masses arise solely from the strong interaction. Glueballs thus offer a unique way to study the mass creation of strongly interacting particles.
How can the unknown structure of glueballs and their properties be addressed and studied? First of all, it would be important to identify and study their behavior as detailed as possible. What criteria do we have to identify glueballs? The experience from previous searches for the scalar glueball tells us that their decay pattern might not be decisive. The scalar glueball with the quantum numbers $J^{PC} = 0^{++}$ is predicted by lattice calculation around at a mass $\approx$ 1.6 GeV/c^2. In the mass region, however, many mesons are present with the same quantum numbers. Mixing between overlapping resonances might occur and destroy a distinctive decay pattern, so the interpretation as glueball is complicated by the mixing of the glueball with the broad light-quark states. But we should have other criteria.
A glueball does not fit into the normal meson nonet with identical quantum numbers, it should be surplus. Glueballs should be produced in so-called gluon-rich reactions like the antinucleon-nucleon annihilation process. The annihilations of the antiquarks with quarks leads to a gluon-rich environment favoring the formation of gluonic degrees of freedom. The central region of a high energetic hadron-hadron scattering process should favor the production of glueballs since it is neither populated by target nor by beam quarks. The radiative decay of quarkonium states and here especially the radiative decay of J/ψ or ψ' mesons should be a prime searching ground for glueballs. Glueballs should not be produced in two photon collisions since gluons do not carry electric charge, which also would suppress their production in a photon beam. The best candidate for the scalar glueball is nowadays the $f_0(1500)$, because it fulfills all of the above criteria.
A consequence of the above mentioned model for glueballs, with the structure of a closed loop of gluonic flux, is the existence of a mass-degenerate glueball state with opposite parity, i.e. a pseudoscalar glueball $J^{PC} = 0^{-+}$. Indeed, the experimental data provide evidence for such a glueball. The particle usually noted as $\eta(1440)$ may indeed be two particles, which are called $\eta(1405)$ and $\eta(1475)$. Especially the $\eta(1405)$ has a strong affinity to glue [38].
We should now see, if the $\eta(1405)$ fulfills our criteria for being a glueball in a similar way as the $f_0(1500)$. Provided that the $\eta(1295)$ does exist, only one of the two states, $\eta(1405)$ and $\eta(1475)$, could be the first radial excitation of the η'. The strong coupling to kaons make the $\eta(1475)$ the prime candidate for being the strangonium member of the nonet. This would leave the $\eta(1405)$ surplus. The key question to answer is the existence of the $\eta(1295)$.
In the past years we have studied the reaction

$$\gamma p \rightarrow p(\pi^0\pi^0\eta) \rightarrow p(6\gamma) \qquad (2)$$

with the Crystal Barrel detector. All appropriate available beam times were analyzed. The resulting invariant mass spectrum is shown in Fig. 7(a):

A hint for a structure at 1405 MeV/c^2 is visible. Also a structure around $\approx$ 1300 MeV/c^2 is present. Selecting mainly $a_0(980)\pi^0$ events by a mass cut of the $\eta\pi$ system between 900 – 1100 MeV/c^2 makes the structure at 1405 MeV/c^2 more evident (Fig. 7(b)). Recent results from PhD theses of Tobias Triffterer and Cathrina Sowa [42, 43] support the assumption, that the $\eta(1405)$ is produced in γp. Using the data acquired by the CBELSA/TAPS experiment with a liquid hydrogen target in 2013, a relative cross section for the production of $\eta(1405)$ candidates can be calculated to 0.16 ± 0.05 by comparing the data to the η' (see Fig. 11)). To determine if the signal around 1300 MeV/c^2 is the $\eta(1295)$ or the well-known $f_1(1285)$ requires to resolve its spin in a partial wave analysis. However, the existing statistics is not sufficient enough to perform such a partial wave analysis.

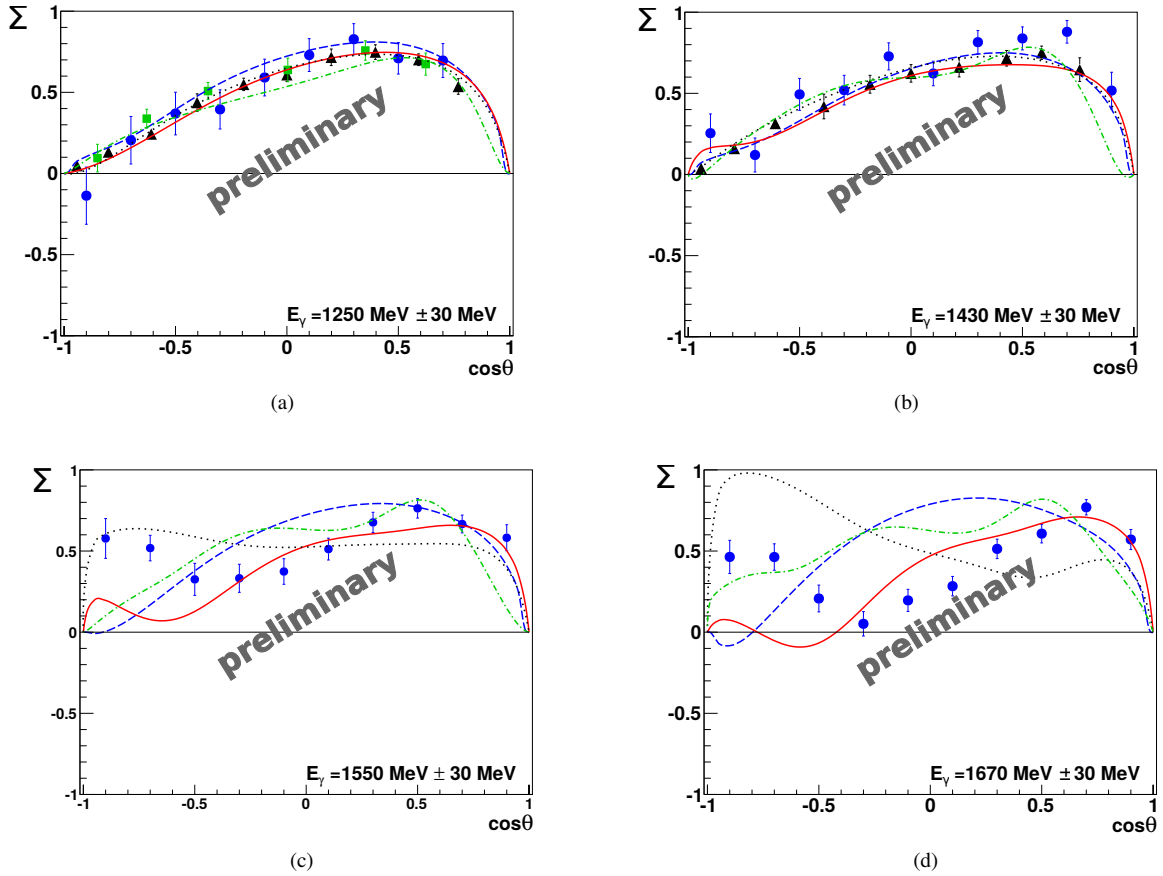

Figure 6. (a)-(d) The beam asymmetry Σ in η-photoproduction is shown for four different energy bins as a function of $\cos\theta_{CMS}$ (blue points) [26]. The data is compared to CB-ELSA data [29] (green squares) and GRAAL data [30] (black triangles) and to the following partial wave analysis solutions: BnGa2014-01 (black dotted line), BnGa2014-02 [35] (red solid line), SAID-GE09 [34] (blue dashed line) and JüBo2015 fit B [32] (green dash-dotted line). (a), (b) and (d) taken from [36].

The recent analysis of the $\eta\pi^+\pi^-$ final state collected by the CLAS collaboration [44] comes to the conclusion, that the mass, width, and an amplitude analysis of the Dalitz distribution are consistent with the axial-vector $f_1(1285)$ identity, rather than the pseudoscalar $\eta(1295)$. The production mechanism is more consistent with s-channel decay of a high-mass N^* state and not with t-channel meson exchange.

For the future, after the successful trigger upgrade of the Crystal Barrel calorimeter (see project D.3) , it is planned to take a dedicated beam time, which will increase the statistics up to two orders of magnitude. This will be sufficient to determine if the $\eta(1405)$ is produced at a cross section comparable to ordinary mesons or with a reduced production cross section, as expected for a glueball. Also, a partial wave analysis will tell us about the existence of the $\eta(1295)$ in the photoproduction process on protons.

While a non-observation, or an observation with suppressed production cross section, in the photoproduction process might serve as indication for the gluonic nature of the $\eta(1405)$, gluon-rich reactions should contain a significant number of $\eta(1405)$ if it has a strong gluonic component. We have studied therefore in the past years in parallel the production of $\eta(1405)$ and $\eta(1295)$ in antiproton-proton annihilations at different energies and radiative charmonia decays.

The BESIII experiment in Beijing has taken in recent years several hundred million J/ψ and ψ' data on resonance. We have looked at gluon-rich radiative decay channels:

$$J/\psi \to \gamma(\pi\pi\eta) \quad \text{and} \quad \psi' \to \gamma(\pi^+\pi^-\eta) \qquad (3)$$

The invariant mass spectra (Fig. 8(a) and 8(b)) show a signal around 1400 MeV/c^2, which contains in case of the J/ψ decays much more events than the signal at $\approx$ 1300 MeV/c^2. This is in sharp contrast to our observations with the photoproduction data. Why the ψ' data look different in the relative ratios between 1405 and 1300 is currently not understood, but certainly worth investigating further. A partial wave analysis of the BESIII data to determine the spin composition of the particles at the respective masses is underway.

Adding additional questions on the nature of the $\eta(1405)$ does another paper published recently by the BES collaboration. In this paper, for the first time the observation of the decay mode of the $\eta(1405)$ into $f_0(980)\pi$ is reported, at a rate completely unexpected by theory [39]. Previous data show that in antiproton-proton annihilations

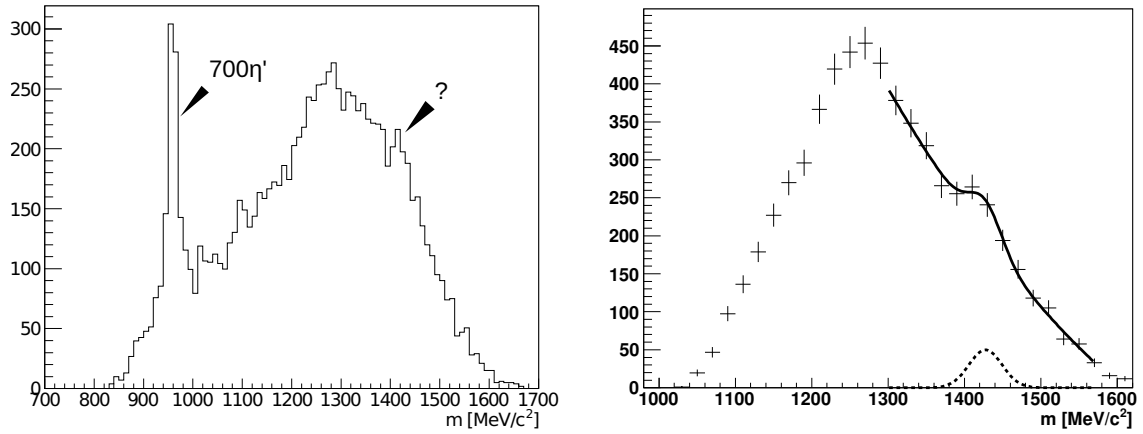

(a) (b)

Figure 7. (a) The $\pi^0\pi^0\eta$ invariant mass spectrum in photon-nucleon reactions for $E_{CM} - m_p > 1450$ MeV with Crystal Barrel at ELSA. (b) The $\pi^0\pi^0\eta$ invariant mass spectrum in photon-nucleon reactions with Crystal Barrel at ELSA requiring that the $\pi^0\eta$ mass is in the $a_0(980)$ (900 MeV< $m(\pi^0\eta)$ < 1100 MeV) mass region.

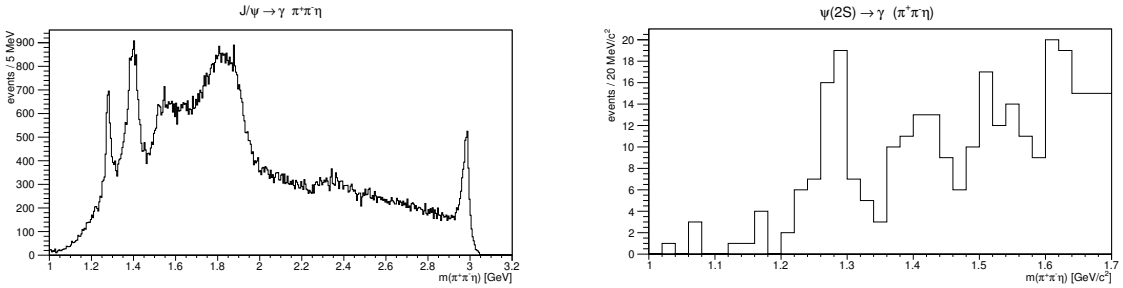

(a) (b)

Figure 8. (a) The $\pi^+\pi^-\eta$ invariant mass in radiative J/ψ decays measured with the BESIII experiment. (b) The $\pi^+\pi^-\eta$ invariant mass in radiative ψ' decays measured with the BESIII experiment.

at rest there is clear evidence that both states, $\eta(1405)$ and $\eta(1475)$, are produced [40, 41]. The $\eta(1405)$ has decay channels both into up and down quark mesons and into strange quark mesons, as expected from a glueball, while the $\eta(1475)$ decays mainly into open strange mesons. These were data at rest and we have now started to look for excited η states in Crystal Barrel data at LEAR from annihilations at 900 and 1800 MeV/c antiproton momentum to study any dependence on the participating initial waves.

The statistics is again rather low, as could be seen in the invariant mass spectra. Nevertheless indications for the presence of signals round 1300 and 1405 MeV/c^2 are there (Fig. 9 and Fig. 10).

To summarize: The comparison between the photoproduction process, radiative charmonia decays and antiproton-proton annihilations shows that the signals at $\approx$ 1300 MeV/c^2 and $\approx$ 1400 MeV/c^2 are produced with very different ratios. The $\approx$ 1400 MeV/c^2 signal in the photoproduction process still needs confirmation in the upcoming years by new data. Partial wave analyses will show if the $\eta(1295)$ is present in the $\approx$ 1300 MeV/c^2 signal or if it is due to the $f_1(1285)$. Such a partial wave analysis, crucial for the interpretation of the data, is currently only possible in the radiative charmonia decays but becomes feasible with higher statistics in the photonuclear reaction with Crystal Barrel experiment.

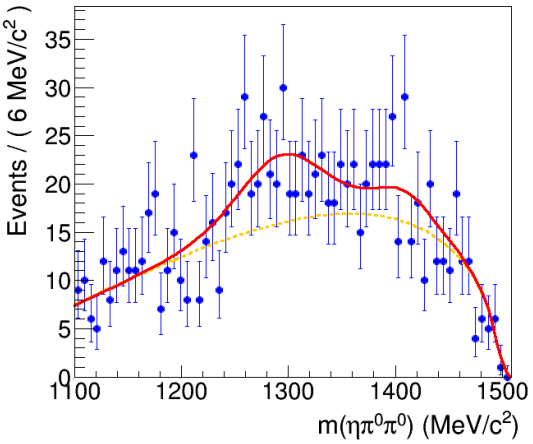

Figure 11. The $\pi^0\pi^0\eta$ invariant mass measured with the CBELSA/TAPS experiment using a liquid hydrogen target in 2013 (blue points) [42]. Additionally, the red curve represents a fit with the hypothesis of $f1(1285)$ and $\eta(1405)$ and the orange curve the background contribution.

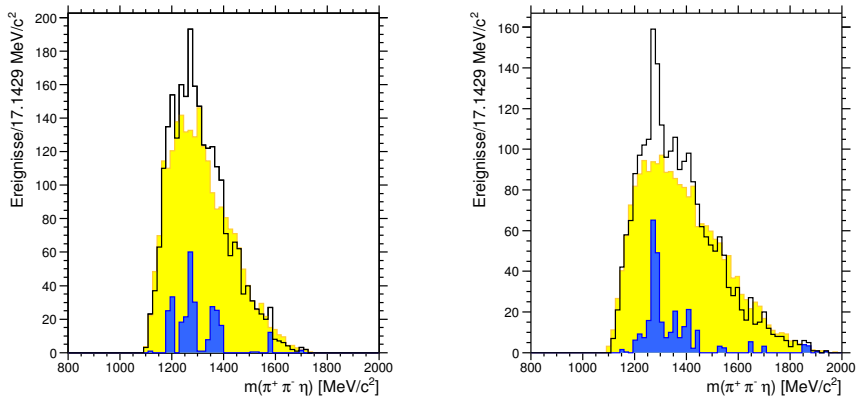

Figure 9. The $\pi^+\pi^-\eta$ invariant mass in antiproton-proton annihilations measured with Crystal Barrel at LEAR. The left side shows data from antiproton momenta of 900 MeV/c and the right side of antiproton momenta of 1642 MeV/c. The non-resonant background calculated by Monte Carlo is shown in yellow and the difference between data and Monte Carlo is shown in blue. Cuts on the invariant $\pi\eta$ mass requiring the events to be within an $a_0(980)$ mass window are applied.

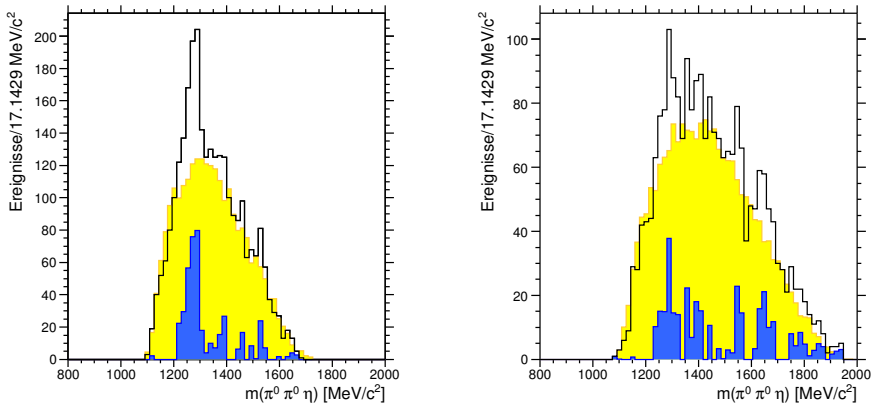

Figure 10. The $\pi^0\pi^0\eta$ invariant mass in antiproton-proton annihilations measured with Crystal Barrel at LEAR. The left side shows data from antiproton momenta of 900 MeV/c and the right side of antiproton momenta of 1642 MeV/c. The non-resonant background calculated by Monte Carlo is shown in yellow and the difference between data and Monte Carlo is shown in blue. Cuts on the invariant $\pi\eta$ mass requiring the events to be within an $a_0(980)$ mass window are applied.

3 Outlook

After the successful trigger upgrade of the Crystal Barrel calorimeter (see project D.3), we plan to have a dedicated beam time with the ELSA tagged photon beam at the highest energies to produce a large η' event sample, to study the η' decays and the $\eta(1405)$ excitation. The cross section for the reaction $\gamma p \rightarrow p\eta'$ lies in the vicinity of 1 μb. The Crystal Barrel is a calorimeter with a wide range in energy and delivers in combination with the TAPS forward wall a solid angle coverage of up to $\Omega = \varepsilon_\Omega \cdot 4\pi$ sr with $\varepsilon_\Omega = 0.98$. The photon beam is produced via the bremsstrahlung process on a thin iron radiator of typical 50 μm thickness. For the reaction $\gamma p \rightarrow p\eta'$ we intend to measure in a photon energy interval from 1.4 GeV to 3.0 GeV expecting an average cross section of $\sigma_T = 1\,\mu$b. By increasing the beam current of the accelerator ELSA and by disabling tagger channels outside the energy range of interest, the integral flux of photons can be increased by a factor of 3 so that the photon flux in the energy range ($\Delta\omega$) between 1400 MeV and 3000 MeV yields $\dot{N}_\gamma(\Delta\omega) = 6 \cdot 10^6\ \gamma$/s.
As target, we intend to use liquid hydrogen in a cylindrical capton container of a length of $l = 10.2$ cm. The target density can be calculated using

$$N_T = \rho_\mathrm{H} l N_A / A\,, \tag{4}$$

where N_T represents the target density, $\rho_\mathrm{H} = 0.0708$ g/cm^3 as the specific density of liquid hydrogen, $N_A = 6.022 \cdot 10^{23}$ mol^{-1} as the Avogadro number and the atomic mass $A = 1.00794$ g/mol. This yields $N_T = 4.315 \cdot 10^{23}$ 1/cm^2. The total rate of produced η' for this set up can be calculated according to

$$\dot{N}_{\eta'} = \dot{N}_\gamma \cdot N_T \cdot \sigma_{\eta'}\,. \tag{5}$$

This yields for $\dot{N}_{\eta'} = 2.589$ s^{-1} over the given 1.6 GeV range between 1400 MeV and 3000 MeV for the total

cross section. This results in a total rate of η' per hour

$$\dot{N}_{\eta'} = 9\,320\,\frac{\text{events}}{\text{h}}\,, \tag{6}$$

According to the branching ratios for η' decays published by the PDG we expect for the six most dominant modes:

Table 1. The branching ratios and number of η' per hour or 1000 h are listed for the most dominant η' decay modes.

Mode	Fraction	$\frac{N_{\eta'}}{\text{h}}$	$\frac{N_{\eta'}}{10^3\text{h}}$
$\pi^+\pi^-\eta$	43.2 ± 0.7 %	4 026	4 026 240
$\rho^0\gamma$	29.3 ± 0.5 %	2 730	2 730 760
$\pi^0\pi^0\eta$	21.7 ± 0.8 %	2 022	2 022 440
$\omega\gamma$	2.75 ± 0.22 %	256	256 300
$\gamma\gamma$	2.22 ± 0.08 %	206	206 904
Total	99.17 %	9 240	9 242 644

The first column of Tab. 1 shows the decay branch, the second column gives the branching ratio, the third column represents the rate of the η' per hour and the fourth column represents the number of η' that can be produced in 1 000 hours of beam time. The sum of "rare" η' decay modes starting with the $\pi^0\pi^0\eta$ contribute 26.7% to the total. Already with the current acceptance of the Crystal Barrel setup, which is ∼60 % for the $\gamma\gamma$ and ∼17 % for the $\pi^0\pi^0\eta$ decay mode, we expect 467 events/h.

The work reported here would not have been possible without the enduring enthusiasm of many bachelor, master, and PhD students and the continuous technical support from staff members of the participating Universities. The support of the ELSA staff members and the polarized target group is gratefully recognized. We would like to thank F. Afzal for contributions to this report. We appreciate the support of the Schweizerischer Nationalfonds, the US National Science Foundation, and the Russian Foundation for Basic Research, in particular the generous support from the Deutsche Forschungsgemeinschaft (SFB/TR16).

References

[1] M. Unverzagt, PhD thesis HISKP, University Bonn (2008).
[2] M. Unverzagt et al., Eur. Phys. J. A **39**, 169 (2009).
[3] S. Prakhov et al., Phys. Rev. C **79**, 035204 (2009).
[4] S. P. Schneider, B. Kubis and C. Ditsche, JHEP **1102**, 028 (2011).
[5] K. Kampf, M. Knecht, J. Novotny and M. Zdrahal, Phys. Rev. D **84**, 114015 (2011).
[6] P. Guo, I. V. Danilkin, C. Fernández-Ramírez, V. Mathieu and A. P. Szczepaniak, arXiv:1608.01447 [hep-ph].
[7] G. Colangelo, S. Lanz, H. Leutwyler and E. Passemar, arXiv:1610.03494 [hep-ph].
[8] A. Nikolaev, PhD thesis HISKP, University Bonn (2011).
[9] A. Nikolaev et al., Eur. Phys. J. A **50**, 58 (2014).
[10] H. Herminghaus et al., Nucl. Inst. Meth. A **138**, 1 (1976).
[11] Th. Walcher, Prog. Part. Nucl. Phys. **24**, 189 (1990).
[12] A. Jankowiak, *Compilation of: Measurement of the electron beam energy at the Mainz Microtron*, MAMI Internal Report 03/2006, Institut für Kernphysik, Mainz (2006).
[13] A. Jankowiak, Eur. Phys. J. A **28**, 149 (2006).
[14] I. Anthony et al., Nucl. Inst. Meth. A **301**, 230 (1991).
[15] S. J. Hall et al., Nucl. Inst. Meth. A **368**, 698 (1996).
[16] A. Reiter et al., Eur. Phys. J. A **30**, 461 (2006).
[17] M. Oreglia et al., Phys. Rev. D **25**, 2259 (1982).
[18] A. Starostin et al., Phys. Rev. C **64**, 055205 (2001).
[19] D. Watts, *Calorimetry in Particle Physics: Proceedings of the 11th International Conference, Perugia, Italy, 2004*, edited by C. Cecchi, P. Lubrano, M. Pepe (World Scientific, Singapore), 560 (2005).
[20] R. Novotny, IEEE Trans. on Nucl. Sc. **38**, 392 (1991).
[21] P. Nuhn, Diploma thesis HISKP, University Bonn (2012).
[22] F. N. Afzal, Master thesis HISKP, University of Bonn (2012).
[23] F. N. Afzal, EPJ Web of Conferences **73**, 04005 (2014).
[24] V. Crede et al., Phys.Rev. C**80**, 055202 (2009).
[25] M. Dugger et al., Phys.Rev.Lett. **96**, 062001 (2006).
[26] F. N. Afzal, PhD thesis HISKP, University of Bonn (2017).
[27] F. Huang et al., arXiv:1208.2279v1.
[28] L. Tiator, Int.J.Mod.Phys. A **22**, 297 (2007).
[29] D. Elsner et al., Eur. Phys. J. A **33**, 147 (2007).
[30] O. Bartalini et al., Eur. Phys. J. A **33**, 169 (2007).
[31] A. V. Anisovich et al., arXiv:1503.05774 [nucl-ex].
[32] D. Rönchen et al., Eur. Phys. J. A **51**, 70 (2015).
[33] R. L. Workman, M. W. Paris, W. J. Briscoe, I. I. Strakovsky, Phys. Rev. C **86**, 015202 (2012).
[34] SAID: http://gwdac.phys.gwu.edu/
[35] E. Gutz et al., Eur. Phys. J. A **50**, 74 (2014).
[36] F. N. Afzal, JPS Conf. Proc. **10**, 032006 (2016).
[37] P. Levi Sandri et al., Eur.Phys.J. A**51**, no.7,77 (2015).
[38] M. Bargiotti et al., Phys. Rev. D **65**, 012001 (2002).
[39] M. Ablikim et al., Phys. Rev. Lett. **108**, 182001 (2012).
[40] C. Amsler et al., Phys. Rev. D **66**, 058101 (2002).
[41] C. Amsler et al., Phys. Lett. B **358**, 389 (1995).
[42] T. Triffterer, PhD thesis, University of Bochum (2016).
[43] C. Sowa, PhD thesis, University of Bochum (2016).
[44] R. Dickson, R. A. Schumacher et al., Phys. Rev. C **93**, 065202 (2016).